Development from Alloys to Nanocomposite for an Enhanced Mechanical and Ignition Response in Magnesium

Khin Sandar Tun [1], Tan Yan Shen Brendan [1], Sravya Tekumalla [2] and Manoj Gupta [1,*]

1 Department of Mechanical Engineering, Faculty of Engineering, Kent Ridge Campus, National University of Singapore, Singapore 637551, Singapore; mpekhst@nus.edu.sg (K.S.T.); Tanyanshenbrendan@gmail.com (T.Y.S.B.)
2 College of Engineering, School of Mechanical and Aerospace Engineering, Nanyang Technological University, Singapore 637551, Singapore; sravya.tekumalla@ntu.edu.sg
* Correspondence: mpegm@nus.edu.sg; Tel.: +65-6516-6358

Abstract: The current study reports on the evolution of microstructure, variations in compressive properties and the ignition resistance of Mg through compositional variation, using alloying elements and nanoreinforcement. The alloys were designed with the use of a singular alloying element, Ca, and a binary alloying element, Ca+Sc, to develop Mg1Ca (wt.%) and Mg1Ca1Sc (wt.%) alloys. B_4C nanoparticles were added as the reinforcement phase in the Mg1Ca1Sc alloy to create the Mg1Ca1Sc/1.5B_4C (wt.%) nanocomposite. The most effective compressive properties and level of ignition resistance was displayed by the developed composite. The grain sizes were significantly reduced in the Mg alloys (81%) and the composite (92%), compared with that of the Mg. Overall, the microstructural features (i.e., grain refinement, the formation of favorable intermetallic compounds, and hard reinforcement particles with an adequate distribution pattern) enhanced both the compressive strength and strain of the alloys and the composite. The ignition resistance was progressively increased from the alloys to the nanocomposite, and a peak ignition temperature of 752 °C was achieved in the composite. When compared with the ignition resistant of Elektron 21 (E21) alloy, which met the Federal Aviation Administration (FAA) requirements, the Mg1Ca1Sc/1.5B_4C nanocomposite showed a higher specific yield strength and better ignition resistance, asserting it as a potential candidate material for lightweight engineering applications, including aerospace and defense sectors.

Keywords: magnesium alloys; composite; grain refinement; ignition temperature; compressive properties

1. Introduction

Due to the concerns surrounding global warming in modern times, there is a significant need to reduce the global levels of carbon dioxide emissions. Moreover, there has been a recent lift in the ban of magnesium-based materials in aircrafts by the Federal Aviation Administration (FAA). Given that magnesium has similar mechanical properties to aluminum, which is commonly used in aircrafts, this allows for a reduction in weight of the aircraft of up to 28% to 30%, should the aluminum components—such as those in the seat elements—be replaced with magnesium [1]. Due to the reduction in the weight of the aircraft, the aircraft would be able to consume less fuel per trip. This not only reduces carbon dioxide emissions, which reduces the carbon footprint of the aviation industry, but also reduces the operating costs of the aviation industry by consuming less fuel.

To be suited to targeted structural applications, the mechanical properties of pure Mg have been continuously enhanced by alloying and composite technologies. To be applicable in the aviation industry, magnesium-based materials must possess not only enhanced mechanical properties, but also enhanced ignition properties. It is necessary to choose promising alloying elements and reinforcement particles which can satisfy the required mechanical and ignition properties. Commercially available Mg alloys such as

Mg–Al–Zn alloys (AZ series magnesium alloys) are widely used in various structural applications, due to their suitable mechanical properties. Although the use of the alloying element Al can improve the alloys' mechanical properties, it is not effective in improving the ignition resistance of magnesium [2–4]. One of the reasons for the occurrence of a low ignition temperature in Al-containing Mg alloys is due to the formation of a low-melting-temperature phase, $Mg_{17}Al_{12}$. The ignition temperature of Mg–Al alloys can be even lower than that of pure Mg [3,4]. In previous studies, the ignition resistance of AZ series magnesium alloys has been seen to increase using Ca as an additional alloying element [5–8]. The addition of Ca can contribute to the increase in ignition temperature in the Mg–Al alloy by increasing the formation of the CaO oxide layer, consequently increasing the onset melting temperature of the $Mg_{17}Al_{12}$ phases and the formation of the thermally stable Al_2Ca phases [6,7]. In addition, the use of Ca also assists in the further improvement of mechanical properties in the base Mg alloy. Generally, the improved mechanical properties in calcium-containing Mg alloys occurs through microstructure evolution, such as grain refinement and secondary phase formation [9–12]. Besides Ca, rare earth elements (REs) are reported as excellent ignition-resistance enhancers [2]. Although the addition of REs can improve the stability of the oxide layer and the ignition resistance of the Mg alloys, the oxidation resistance and ignition behaviour of the alloys strongly depend on the alloy composition, microstructure, and solubility limit of alloying elements (REs). Zhao et al. [13] reported a decrease in the ignition resistance of the AZ91D/Nd alloy with the use of low Nd content at 0.5 wt.%; however, an increase in the ignition temperature was noted with the use of high Nd content at 5 wt.%. On the other hand, a decrease in the ignition temperature of the Mg alloys containing REs such as La, Pr, and Ce, which have very low solid solubility in Mg, was also reported [3].

The aim of the current study was to use Ca as an alloying element for the improvement of both mechanical and ignition properties. Due to the important role of Ca in increasing the ignition temperature and high-temperature oxidation resistance of Mg, calcium-containing magnesium-based alloys and composites have been designed systemically. In our study, Ca was first used as singular alloying element in Mg, creating the Mg1Ca (wt.%) alloy. Then, 1 wt.% Sc was added as an additional alloying element into the Mg1Ca alloy, to study the combined effect of Ca and Sc, with the expectation that it would enhance the mechanical and ignition properties of the Mg1Ca1Sc alloy. A favorable ignition response was projected from the alloy, considering the high solubility limit (~16 at.%) of Sc in Mg [14]. Finally, B_4C nanoparticle reinforcement was added into the Mg1Ca1Sc alloy to develop the Mg alloy composite. The selection of B_4C for the reinforcement phase was based on previous studies [15,16] which have reported the advantages of using this reinforcement phase in improving the mechanical and ignition properties of Mg and Mg alloys.

2. Processing and Characterization

The Mg alloys and composite (Mg1Ca and Mg1Ca1Sc and Mg1Ca1Sc/1.5B_4C) were synthesized using the disintegrated melt deposition (DMD) technique. The compositions used for the alloys and composite were in weight percentage; magnesium turnings (>99.9% purity, ACROS Organics, Morris Plains, NJ, USA), Mg-30Sc master ingots (99.9% purity, Sunrelier Metal Company Shanghai, China), Calcium granules (99.8% purity, Alfa Aesar, Massachusetts, United States) and B_4C nanoparticles of ~50 nm size (Nabond, Shenzhen,, China) were used as raw materials for the materials preparation. The raw materials were weighed in accordance with the designated compositions and placed in a graphite crucible. The materials were heated to 750 °C using an electrical resistance furnace in an atmosphere of inert argon gas. The molten melt was poured through a nozzle of 10 mm diameter at the bottom of the crucible, to the mold below the crucible. Two jets of argon gas, oriented normal to the melt stream, were used to disintegrate the molten metal before it entered the mold. The disintegrated melt was then deposited into the cylindrical mold of 40 mm diameter. This ingot was later machined to 36 mm diameter and used for the secondary process of extrusion. The cast ingot was homogenized at 400 °C for 1 h, followed by hot

extrusion at 350 °C, using a 150-tonne hydraulic extrusion press The extrusion ratio of 20.25:1 was used to obtain the extruded rods of 8 mm.

Microstructural characterization was performed using a JEOL JSM-6010 scanning electron microscope (JEOL Ltd., Tokyo, Japan), equipped with energy dispersive X-ray analysis (EDX, JEOL Ltd., Tokyo, Japan), to analyze the grain size, phase morphology, phase compositions, and distribution pattern of grains and secondary phases in the developed materials. MATLAB analysis software (R2013b, MathWorks, Massachusetts, USA) was used to measure the grain size in the Mg alloys and the composite. The room temperature compressive tests were performed on the samples in conformation with the procedures detailed in the Standard ASTM E9-89a, using a fully automated MTS810 servo-hydraulic test machine (MTS systems corporation, Eden Prairie, MN, USA). Cylindrical samples with a length to diameter ratio of 1 were used for compressive testing. The ignition temperatures of the materials were determined using a Thermo Gravimetric Analyzer (TGA, Netzsch Selb, Germany). Samples with dimensions of approximately 2 mm × 2 mm × 1 mm were placed in purified air with a flow rate of 50 mL/min. They were heated from 30 to 1000 °C at a heating rate of 10 °C/min. A graph of temperature vs. time was obtained from the test. The point at which the rapid change in temperature was observed in the graph was recorded as the ignition temperature of the materials.

3. Results and Discussion

3.1. Microstructure Evolution in Alloys and Composite

Figure 1 represents the microstructures of the alloys and composite. The presence of secondary phases was analyzed through EDX analysis, as shown in Figure 2. Based on the Mg–Ca binary phase diagram [17], there was very low solid solubility of Ca in Mg (0.82 at.%). Consequently, the formation of Mg_2Ca is a common finding in calcium-containing Mg alloys [9–12]. In the present study, the formation of the intermetallic compound, Mg_2Ca, was also observed in the alloys Mg1Ca and Mg1Ca1Sc, and the composite Mg1Ca1Sc/B_4C. The presence of the Mg_2Ca phase was confirmed through elemental analysis, using EDX as seen in Figure 2. As shown in Figure 1a, the Mg_2Ca phases were uniformly distributed in the extruded Mg1Ca alloy, with minimal presence of clusters. Following the addition of Sc as an additional alloying element in the Mg1Ca1Sc alloy and its composite, the formation of the Mg–Sc phase [18], together with the Mg_2Ca phases, can be seen in the micrographs in Figure 1b,c and Figure 2b,c. Through the EDX mapping results shown in Figure 3, the fine phases were confirmed to be the Mg_2Ca phase and coarse phase was confirmed as the Mg–Sc phase. The tendency for the clustering of phases was relatively higher in the Mg1Ca1Sc alloy compared with the Mg1Ca alloy. In the composite, besides the presence of the Mg_2Ca and Mg–Sc phases, the reinforcement particles B_4C can be seen in the micrograph in Figures 1c and 2c. From the EDX analysis in Figure 2c, it can be seen that the element B was not detected, but a low intensity peak of carbon, C, was found instead. This indicates the presence of B_4C in the composites. The elemental information of B and C was not strong enough to pick up through the EDX analysis, due to very fine and dispersed reinforcement particles (Figures 1c and 2c).

From the composite's microstructure (Figures 1c and 2c), the clustered phases were reduced and a fine dispersion of Mg_2Ca and B_4C particles could be found. Overall, the distribution pattern of the secondary phases, Mg_2Ca, Mg–Sc and B_4C, was homogeneous in the composite material.
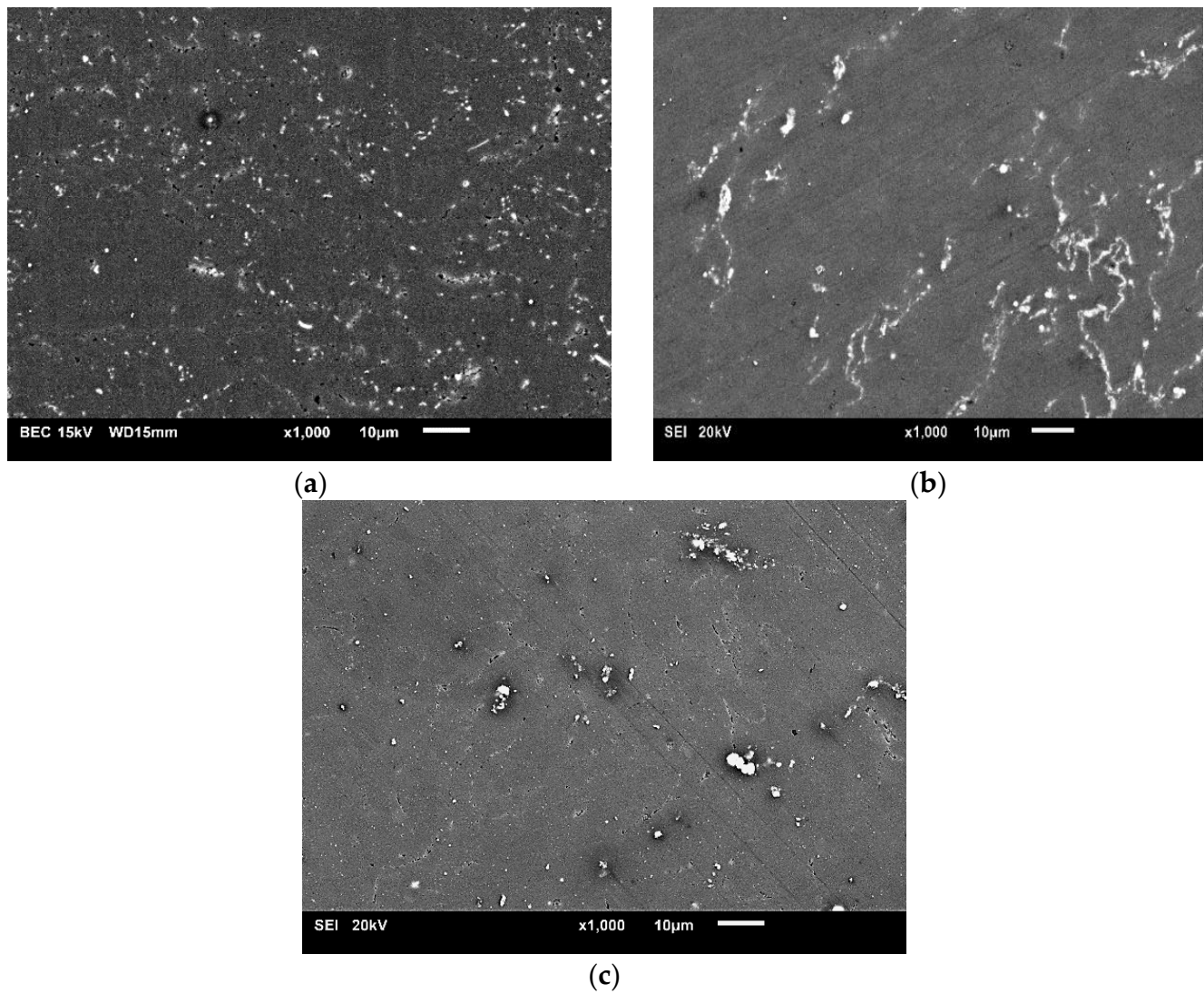
Figure 1. Formation, distribution, and morphology of secondary phases in: (**a**) Mg1Ca alloy, (**b**) Mg1Ca1Sc alloy, and (**c**) Mg1Ca1Sc/B₄C composite.
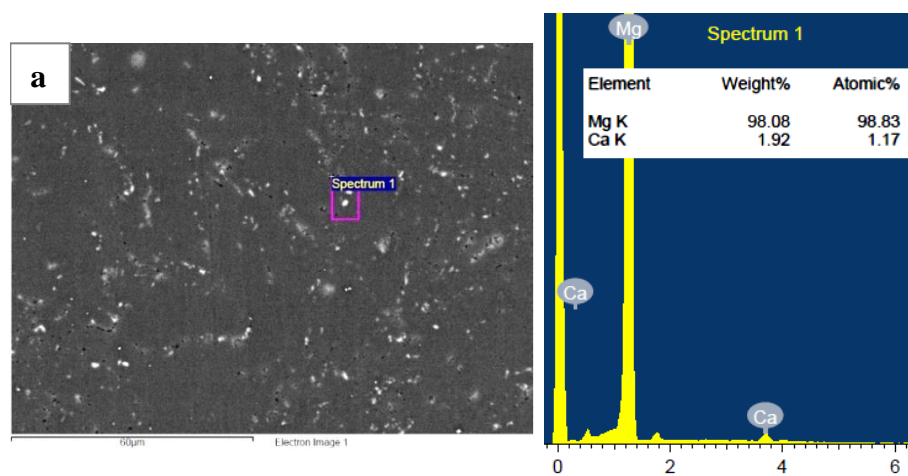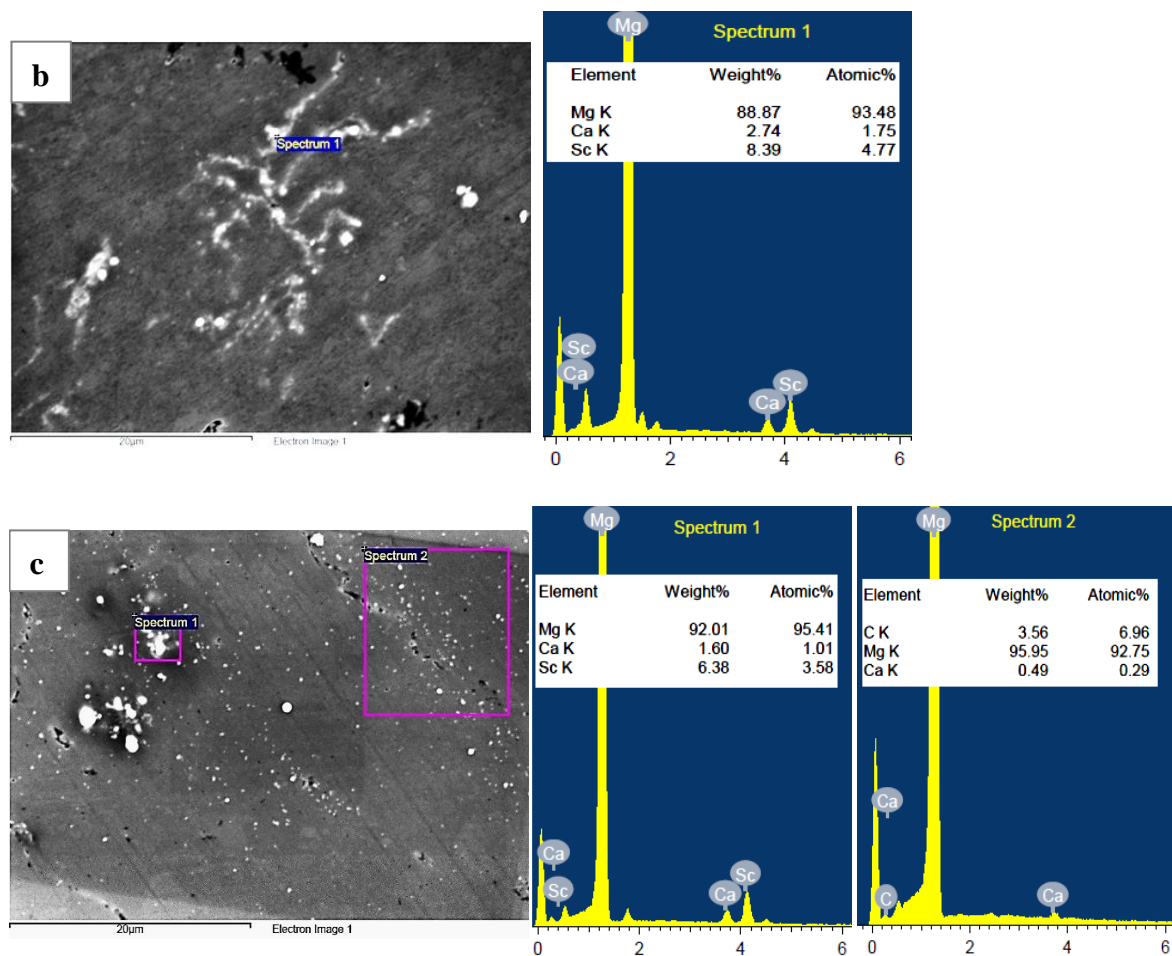

Figure 2. *Cont.*

Figure 2. EDX analysis showing: (**a**) Mg and Ca peaks in Mg1Ca alloy, (**b**) Mg, Ca and Sc peaks in Mg1Ca1Sc alloy and (**c**) Mg, Ca, Sc and C peaks in Mg1Ca1Sc/1.5B$_4$C composite.
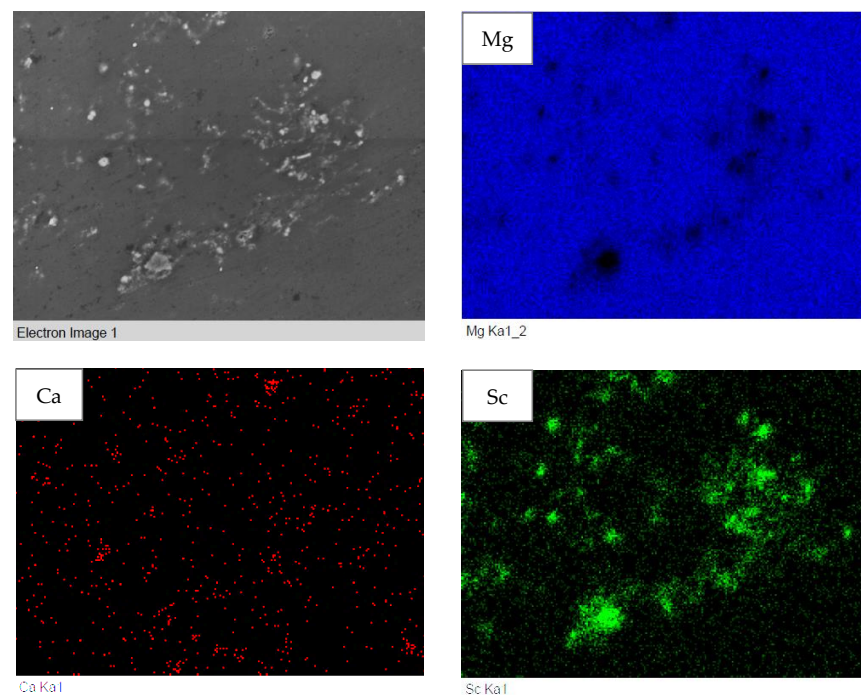

Figure 3. EDX mapping analysis of the Mg1Ca1Sc alloy.

3.2. Grain Morphology/Distribution

Figure 4 shows the SEM micrographs presenting a comparison of grain sizes in pure Mg, Mg alloys and the composite. The micrographs were taken along the extrusion direction. All materials revealed a relatively homogeneous grain structure, a nearly equiaxed grain morphology, and the absence of any elongated grains along the extrusion direction. These observations indicated that the grains were fully recrystallized in all extruded materials. As shown in the grain distribution patterns in Figure 4, the alloys and the composite demonstrated a better homogeneous grain size distribution, compared with pure Mg. The average grain sizes were measured to be 21 ± 6 μm, 4 ± 1 μm, 4 ± 1 μm and 1.7 ± 0.4 μm for Mg, the Mg1Ca and Mg1Ca1Sc alloys and the Mg1Ca1Sc/B_4C composite, respectively. The use of alloying elements, Ca and Ca+Sc in Mg led to a significant grain size reduction in their respective alloys, Mg1Ca and Mg1Ca1Sc, indicating the effectiveness of the selected alloying elements. However, the combined presence of Ca and Sc in the Mg1Ca1Sc alloy did not cause a further reduction in grain size, resulting in the same average grain size as in the Mg1Ca alloy. This can be explained through microstructural observation.

Dynamic recrystallization takes place during deformation, such as during the hot extrusion of the materials. The presence of either mixed grain sizes (coarse grains and fine grains) or elongated grains along the extrusion direction are indicative of incomplete recrystallization. In the current investigation, near equiaxed grains, together with their uniform distribution pattern observed in all the materials, indicated that full recrystallization happened via dynamic recrystallization during hot extrusion (Figure 4). For magnesium-based materials containing certain types of intermetallic compounds or reinforcement particles (secondary phases), those phases can act as the source to stimulate the recrystallization process. The nucleation of new grains occurs at the deformation zone around hard secondary phases, or particles during hot extrusion, which is generally known as particle-stimulated nucleation (PSN). In the microstructure of the Mg1Ca alloy (Figures 1a and 2a), well distributed Mg_2Ca phases can be seen. A remarkable grain size reduction of 81% was observed in the Mg1Ca alloy, compared with Mg, and therefore the potential capability of the Mg_2Ca phases to play a critical role in the grain refinement of Mg through particle-stimulated dynamic recrystallization during hot extrusion is envisaged. When compared with the Mg1Ca alloy, the same average grain size, as well as a similar grain distribution pattern, was observed in the Mg1Ca1Sc alloy (Figure 4b,c). As seen in the microstructure of the Mg1Ca1Sc alloy, the addition of Sc to the Mg1Ca alloy caused the increased clustering (Mg_2Ca + Mg–Sn) of secondary phases (Figure 2b), while maintaining the distribution pattern of Mg_2Ca phases based on the EDX analysis in Figure 3. This meant that the distribution pattern of the secondary phases between the Mg1Ca and Mg1Ca1Sc alloys was the same, and the formation of the additional Mg–Sc phases only caused clustered phases. Further grain refinement would only be possible if there was a balance between the increased second phases and their relative uniformity of distribution [19,20]. This explains the lack of further grain refinement in the Mg1Ca1Sc alloy. In the case of the Mg1Ca1Sc/B_4C composite, the particle reinforcement caused a 58% reduction in grain size in relation to the Mg1Ca1Sc alloy, and 92% reduction in relation to Mg. This clearly shows that the fine B_4C particulates had a strong capability in grain growth restriction through the classical grain-boundary pinning mechanism [15,16]. In addition, the homogeneous grain-distribution pattern was attained (Figure 4d) as a consequence of microstructural homogeneity, in terms of good second phase distribution in the composite (Figures 1c and 2c).
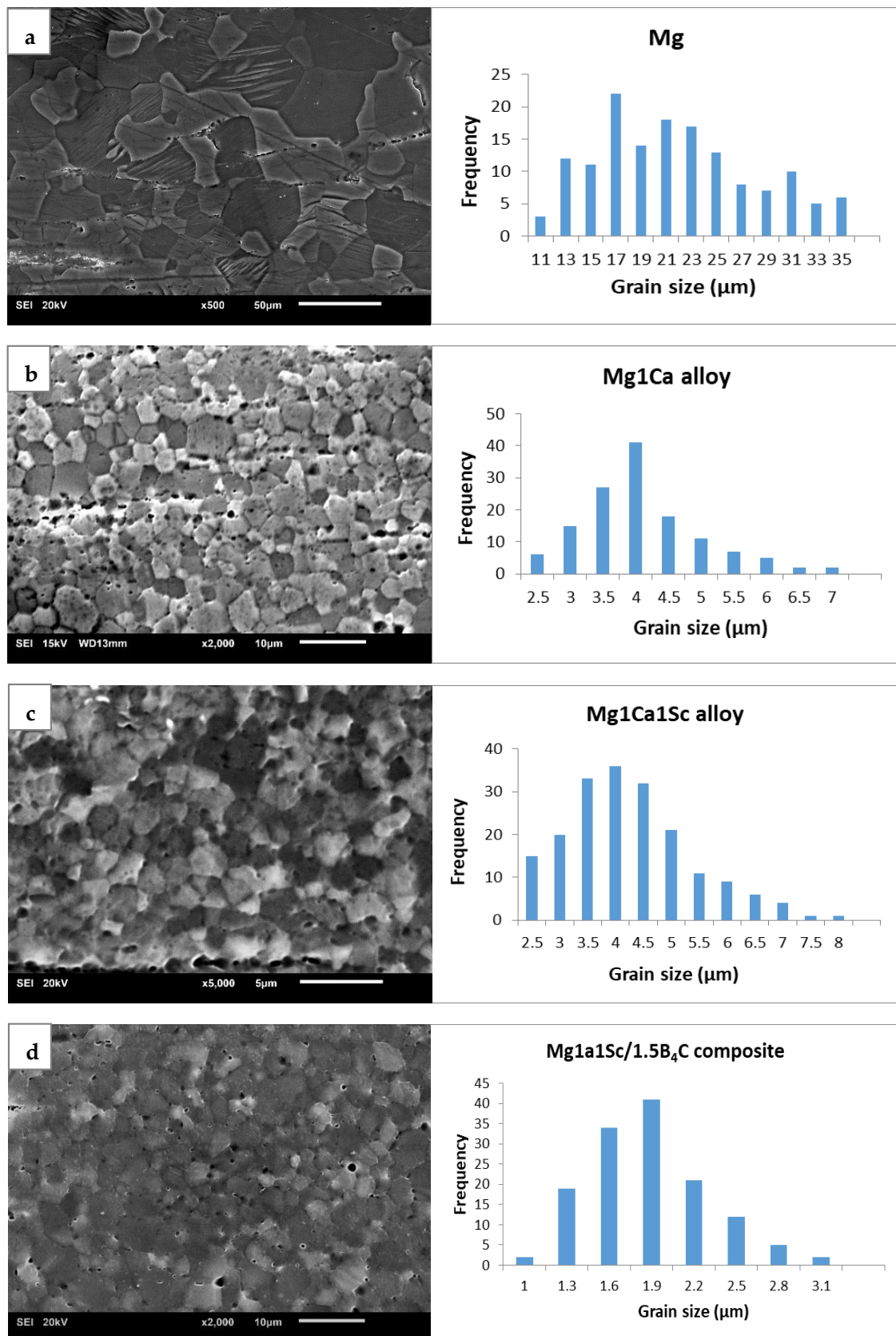
Figure 4. SEM micrographs showing grain sizes and distribution patterns in: (**a**) Mg, (**b**) Mg1Ca alloy, (**c**) Mg1Ca1Sc alloy and (**d**) Mg1Ca1Sc/B_4C composite.

3.3. Ignition Properties

The ignition temperature of magnesium can be increased by alloying and composite methods, using suitable alloying elements and reinforcement materials. The ignition temperatures of the Mg alloys and composite developed in this study are shown in Figure 5. The addition of the alloying element Ca has been proven to increase the ignition properties of Mg [5–8]. The Mg1Ca alloy developed in the current study also showed the improved ignition temperature of 11% over Mg. Generally, the ignition occurs in Mg through two stages: (i) formation of a loose oxide layer (MgO) below 500 °C and (ii) the breakdown of the MgO layer causing the fresh metal, Mg, to be in contact with oxygen. This leads to a high oxidation rate, triggering a rapid increase in surface temperature that is eventually followed by Mg ignition [21,22]. In the Mg1Ca alloy, the additional oxide layer, CaO can be formed beside the MgO formation. Previous studies [3,21] have shown that the MgO oxide layer is thermally unstable at high temperatures (480–500) and results in the formation of the CaO oxide layer in the later stage of oxidation. The formation and nature of the oxide layers in Mg alloys are usually correlated with their ignition properties. From the reported experimental evidence, a more compact and protective CaO layer was formed in the Mg alloys containing the Ca element [3,5,21]. Hence, the improved ignition resistance observed in the current Mg1Ca alloy can be explained based on the additional formation of the protective and thermally stable oxide layer: CaO formation with the use of Ca as an alloying element in Mg.
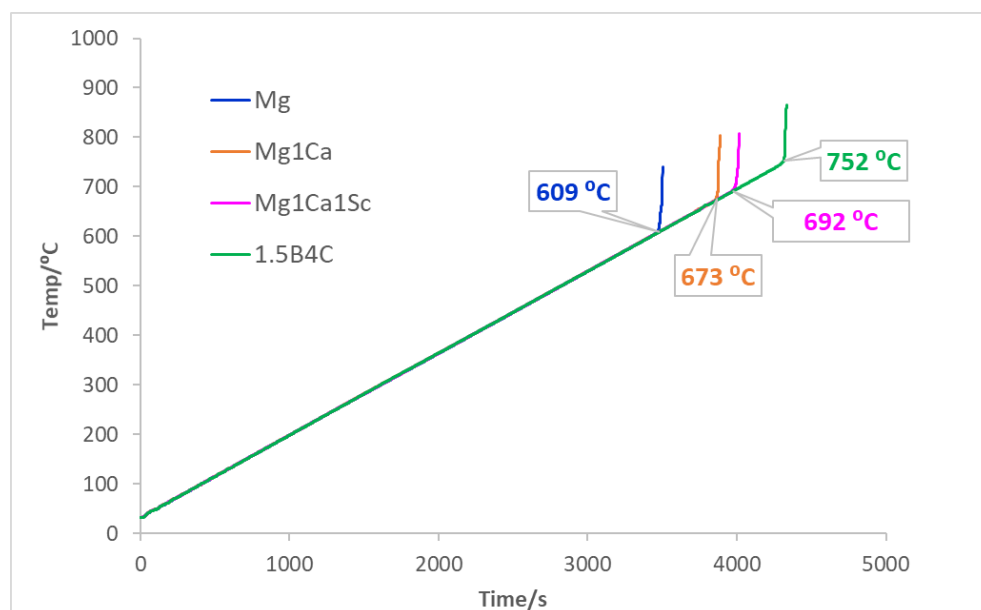

Figure 5. Ignition temperatures of Mg, the Mg alloys and the Mg nanocomposite.

The addition of some rare earth elements such as Y, Gd, Dy, and Er have also proven to enhance the ignition resistance of Mg [2,3]. In the current study, the rare earth element Sc was used as an alloying element in an Mg1Ca alloy. The ignition test results (Figure 5) show the improved ignition temperature in the MgCa1Sc alloy. Kim et al. [3] reported the effect of solid solubility in Mg alloys containing rare earth alloying elements; it was found that Mg–La and Mg–Pr have a low ignition resistance compared with other Mg–RE alloys, which have medium to high solid solubility. In those alloys, solute concentration was increased during heating due to the dissolution of the secondary phases, and those elements contributed to an increase in the alloys' ignition resistance. From the Mg–Sc binary-phase diagram [14], it can be seen that it had a solubility limit of ~16 at.% Sc in Mg. High solute concentration in the Mg1Ca1Sc alloy can be expected, due to the high solid solubility of Sc in the Mg matrix leading to an increase in the ignition temperature. This

indicates the beneficial effect of the Sc addition to the Mg1Ca alloy, with a higher ignition temperature being observed in the Mg1Ca1Sc alloy compared with the Mg1Ca alloy (14%).

Regarding the Mg–Al alloy system, solubility of Al is high in Mg, yet the ignition resistance of the Mg–Al alloy is low [3,4]. The reason for this is due to the formation of thermally unstable secondary phases; this indicates that the presence of thermally stable secondary phases is an important factor to improve ignition resistance. Previous studies on the ignition properties of magnesium-based nanocomposites have shown the enhancement of magnesium's ignition resistance due to the use of thermally stable reinforcements such as B_4C, Sm_2O_3 and CeO_2 nanoparticles [16,23,24]. In the current study, a further increase in ignition temperature from 692 °C in the Mg1Ca1Sc alloy to 752 °C in the Mg1Ca1Sc/B_4C composite was observed (Figure 5). This clearly indicates the effectiveness of the presence of B_4C nanoparticle reinforcements in improving the ignition resistance of Mg alloys.

With regard to microstructural analysis, in terms of grain size and distribution, finer grains and a better distribution of grain sizes were observed in the developed alloys and composite, compared with pure Mg. Grain size variation, as well as the homogeneity of grain size, is correlated to the oxide layer formation, which in turn is related to the ignition properties of the materials. The presence of high density grain boundaries (defects) can promote the formation of oxide film, since the grain boundary is susceptible to easy oxidation [25]. In addition, the differential driving force for oxidation is reduced, due to the availability of uniform grains. Hence, the presence of fine and uniform grains facilitates the formation of stable and protective oxide layers, thereby assisting in promoting the ignition temperature of the currently developed Mg alloys and composite [25,26].

3.4. Compressive Properties

As shown in Table 1 and Figure 6, the compressive properties of Mg were enhanced in the currently developed Mg alloys and nanocomposite. Strength and ductility, namely the compressive yield strength (0.2% CYS), ultimate compressive strength (UCS) and compressive strain were improved in the Mg1Ca, Mg1Ca1Sc alloys and the Mg1Ca1Sc/B_4C nanocomposite when compared with those of pure Mg. The least improvement of 51% CYS, 8% UCS and 23% strain was observed in the Mg1Ca1Sc alloy. Overall, the highest compressive property increment was achieved in the Mg1Ca1Sc/B_4C nanocomposite with an improvement of 111% CYS, 20% UCS and 35% strain. The factors affecting the variation in mechanical properties of magnesium-based materials include the grain size, the size, the amount and morphology of intermetallic compounds or secondary phases and the type and nature of reinforcements used. From the grain size analysis (Figure 4a–c), a significant grain size reduction was observed in the Mg1Ca and Mg1Ca1Sc alloys, compared with Mg. Consequently, the compressive properties of the alloys were increased over pure Mg. Although there was the same average grain size in both alloys, reduced compressive strengths and strain was found in the Mg1Ca1Sc alloy, when compared with the Mg1Ca alloy. In observing the same grain sizes, as well as the similar pattern of grain size distribution, we assumed that there must have been another factor influencing the variation of compression properties between these two alloys. From the microstructure analysis, the distribution pattern of secondary phases in Mg_2Ca was relatively homogeneous throughout the Mg matrix, with the use of a single alloying element, Ca, in the Mg1Ca alloy. In the microstructure of the Mg1Ca1Sc alloy, most of the Mg_2Ca phases were seen clustering with the Mg–Sc phases (Figure 3). This microstructure changed the effects of the compressive properties, thereby observing reduced strength and strain in the Mg1Ca1Sc alloy, compared with the Mg1Ca alloy, despite having the same grain sizes. In the case of the Mg1Ca1Sc/B_4C composite, small clusters of secondary phases (Mg_2Ca + Mg–Sc) were seen in the microstructure (Figures 1c and 2c). In the previous study [27], it was reported that reinforcement nanoparticles possessed the ability to assist in the breakdown of large clusters of secondary phases into small clusters. Similarly, in the present study, coarse secondary phase clusters in the Mg1Ca1Sc alloy were reduced into small clusters, with the addition of nano B_4C particles in the composite material. In addition, the presence of nano

B$_4$C particles did not cause the nanoparticle clustering itself; instead, well distributed B$_4$C were observed with the co-presence of Mg$_2$Ca phases in the Mg matrix (Figure 2c). The combined factors of (i) a further grain size reduction of 58% compared with the Mg1Ca and Mg1Ca1Sc alloys, (ii) microstructural homogeneity in terms of second phase distribution and (iii) the presence of abundant hard phases, led to the highest overall compressive properties in the Mg1Ca1Sc/B$_4$C composite.

Table 1. Compressive properties of the developed Mg alloys and nanocomposite.

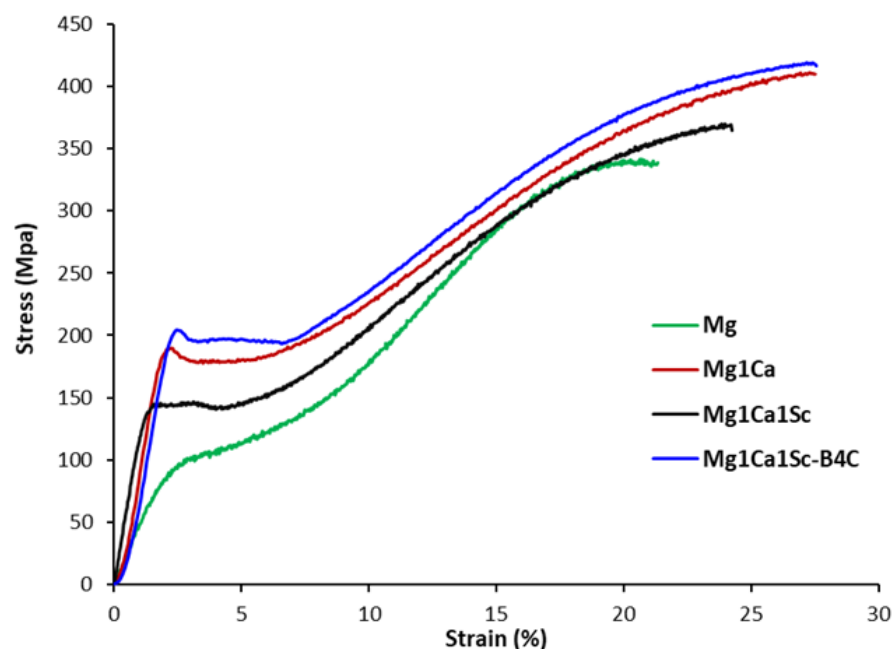| Material	0.2% CYS (MPa)	UCS (MPa)	Compressive Strain (%)
Mg	96 ± 6	342 ± 4	20 ± 1
Mg1Ca	187 ± 9 (95%)	403 ± 14 (18%)	28 ± 1 (40%)
Mg1Ca1Sc	145 ± 7 (51%)	371 ± 2 (8%)	24.6 ± 0.3 (23%)
Mg1Ca1Sc/B$_4$C	203 ± 2 (111%)	410 ± 9 (20%)	27 ± 2 (35%)

Figure 6. Compressive deformation curves of Mg, Mg alloys and the Mg nanocomposite.

Among the commercial Mg alloys, the Elektron 21 (E21) alloy met the requirements and passed the flammability test from the Federal Aviation Administration (FAA). It is highly qualified to be used in the aviation industry [16]. E21 is composed of high-density alloying elements such as Neodymium, Gadolinium, Zinc and Zirconium; its density is similar to the density of the AZ series Mg alloys (~1.8 g/cm^3). In our current composite, low-density alloying elements, Ca (1.55 g/cm^3) and Sc (2.985 g/cm^3) and the reinforcement phase, B$_4$C (2.52 g/cm^3), were used in Mg. Accordingly, the density of the Mg1Ca1Sc/1.5B$_4$C composite was low (1.76 g/cm^3). From the comparison results shown in Table 2, the specific yield strength of the developed composite is higher than the E21 alloy. In addition to its strength, a higher ignition temperature was also accomplished in the composite, compared with E21. Hence, this shows the potential for the Mg1Ca1Sc/1.5B$_4$C composite to be used in the aviation industry. Further testing, such as flammability and standardization by the FAA, is still needed for the currently developed composite to be qualified as an aerospace material.

Table 2. Comparison properties between E21 and the Mg1Ca1Sc/B_4C nanocomposite.

Material	CYS (MPa)	Density (g/cm^3)	Specific Yield Strength (MPa cm^3 g^{-1})	Ignition Temperature (°C)
Mg1Ca1Sc/1.5B_4C	203	1.76	115	752
E21	141	1.8	78	741

4. Conclusions

This study demonstrated the systematic development of Mg alloys, Mg1Ca and Mg1Ca1Sc, to the Mg nanocomposite Mg1Ca1Sc/1.5B_4C. The resultant properties in Mg were due to the addition of a singular alloying element (Ca) and a binary alloying element (Ca+Sc), in addition to the nano B_4C particle reinforcement in the composite. The key points of the study can be summarized as follows:

1. In the Mg1Ca alloy, the uniform distribution of the secondary phases of Mg_2Ca was observed in its microstructure. The clustering of the Mg_2Ca and Mg–Sc phases were seen in the microstructure of the Mg1Ca1Sc alloy. The addition of B_4C nanoparticles to the Mg1Ca1Sc alloy was effective in breaking down those coarse clusters into small clusters in the Mg nanocomposite;
2. Significant grain refinement was seen, with 81% grain size reduction in the Mg alloys and 92% reduction in the Mg composite over pure Mg. A reasonable distribution pattern of secondary phases and/or reinforcement phases led to the grain size homogeneity in the alloys and composite;
3. A progressively higher resistance to ignition was noted with the addition of Ca, Ca+Sc and Ca+Sc+B_4C in the Mg1Ca and Mg1Ca1Sc alloys and the Mg1Ca1Sc/B_4C composite. Hence, the corresponding formation of Mg_2Ca and Mg–Sc phases, and added nanoparticles, were proven to be effective in enhancing the ignition resistance of Mg;
4. Under compressive loading, both strength and ductility were improved in the currently developed Mg alloys and nanocomposite. The highest overall compressive properties were achieved in the Mg nanocomposite due to its microstructural homogeneity (finest grain size, grain size homogeneity and uniform distribution of secondary phases) and increased presence of secondary phases (Mg_2Ca, Mg–Sc and B_4C);
5. It is to be noted that a higher specific yield strength and ignition resistance were also accomplished in the developed nanocomposite, when compared with the aerospace alloy, E21.

References

1. Czerwinski, F. Controlling the ignition and flammability of magnesium for aerospace applications. *Corros. Sci.* **2014**, *86*, 1–16. [CrossRef]
2. Tekumalla, S.; Gupta, M. An insight into ignition factors and mechanisms of magnesium based materials: A review. *Mater. Des.* **2017**, *113*, 84–98. [CrossRef]
3. Kim, Y.M.; Yim, C.D.; Kim, H.S.; You, B.S. Key factor influencing the ignition resistance of magnesium alloys at elevated temperatures. *Scr. Mater.* **2011**, *65*, 958–961. [CrossRef]
4. Takeno, T.; Yuasa, S. Ignition of Magnesium and Magnesium-Aluminum Alloy by Impinging Hot-Air Stream, Combust. *Sci. Technol.* **1980**, *21*, 109–121. [CrossRef]
5. Inoue, S.; Yamasaki, M.; Kawamura, Y. Formation of an incombustible oxide film on a molten Mg-Al-Ca alloy. *Corros. Sci.* **2017**, *122*, 118–122. [CrossRef]
6. Cheng, C.; Lan, Q.; Liao, Q.; Le, Q.; Li, X.; Chen, X.; Cui, J. Effect of Ca and Gd combined addition on ignition temperature and oxidation resistance of AZ80. *Corros. Sci.* **2019**, *160*, 108176. [CrossRef]
7. Cheng, C.; Lan, Q.; Wang, A.; Le, Q.; Yang, F.; Li, X. Effect of Ca Additions on Ignition Temperature and Multi-Stage Oxidation Behavior of AZ80. *Metropolitan* **2018**, *8*, 766. [CrossRef]
8. Cheng, S.; Yang, G.; Fan, J.; Li, Y.; Zhou, Y. Effect of Ca and Y additions on oxidation behavior of AZ91 alloy at elevated temperatures. *Trans. Nonferrous Met. Soc. China* **2009**, *19*, 299–304. [CrossRef]
9. Zhang, E.; Yang, L. Microstructure mechanical properties and bio-corrosion properties of Mg–Zn–Mn–Ca alloy for biomedical application. *Mater. Sci. Eng. A* **2008**, *497*, 111–118. [CrossRef]
10. Du, Y.Z.; Zheng, M.Y.; Qiao, X.G.; Wu, K.; Liu, X.D.; Wang, G.J.; Lv, X.Y.; Li, M.J.; Liu, X.L.; Wang, Z.J.; et al. The effect of double extrusion on the microstructure and mechanical properties of Mg–Zn–Ca alloy. *Mater. Sci. Eng. A* **2013**, *583*, 69–77. [CrossRef]
11. Zhang, B.; Wang, Y.; Geng, L.; Lu, C. Effects of calcium on texture and mechanical properties of hot-extruded Mg–Zn–Ca alloys. *Mater. Sci. Eng. A* **2012**, *539*, 56–60. [CrossRef]
12. Zhou, M.; Huang, X.; Morisada, Y.; Fujii, H.; Chino, Y. Effects of Ca and Sr additions on microstructure, mechanical properties, and ignition temperature of hot-rolled Mg–Zn alloy. *Mater. Sci. Eng. A* **2020**, *769*, 138474. [CrossRef]
13. Zhao, W.M.; Zhao, Y.; Wang, Z.F.; Li, Y.Y.; Ding, J.; Xue, H.T. Effect of Mg-Nd Master Alloys on Ignition-Proof Performance of AZ91D Magnesium Alloy. *Adv. Mater. Res.* **2011**, *214*, 118–121. [CrossRef]
14. Nayeb-Hashemi, A.A.; Clark, J.B. The Mg−Sc (Magnesium-Scandium) system. *Bull. Alloy. Phase Diagr.* **1986**, *7*, 574–578. [CrossRef]
15. Sankaranarayanan, S.; Sabat, R.K.; Jayalakshmi, S.; Suwas, S.; Gupta, M. Effect of nanoscale boron carbide particle addition on the microstructural evolution and mechanical response of pure magnesium. *Mater. Des.* **2014**, *56*, 428–436. [CrossRef]
16. Tekumalla, S.; Yuan, N.J.; Haghshenas, M.; Gupta, M. Enhancing Properties of Aerospace Alloy Elektron 21 Using Boron Carbide Nanoparticles as Reinforcement. *Appl. Sci.* **2019**, *9*, 5470. [CrossRef]
17. Nayeb-Hashemi, A.A.; Clark, J.B. The Ca−Mg (Calcium-Magnesium) system. *Bull. Alloy Phase Diagr.* **1987**, *8*, 58–65. [CrossRef]
18. Dutkiewicz, J.; Rogal, Ł.; Kalita, D.; Fima, P. Development of new age hardenable Mg-Li-Sc alloys. *J. Alloys Compd.* **2019**, *784*, 686–696. [CrossRef]
19. Tun, K.S.; Zhang, Y.; Parande, G.; Manakari, V.; Gupta, M. Enhancing the Hardness and Compressive Response of Magnesium Using Complex Composition Alloy Reinforcement. *Metals* **2018**, *8*, 276. [CrossRef]
20. Sun, J.; Ma, Y.; Miao, H.; Li, K.; Li, C.; Huang, H. Effect of Ca Concentration on Microstructure and Mechanical Properties of As-Cast and As-Extruded Quasicrystal-Strengthened Mg-7.2Zn-2.4Gd Alloy. *Adv. Mater. Sci. Eng.* **2018**, *2018*, 9138753. [CrossRef]
21. You, B.-S.; Park, W.-W.; Chung, I.-S. The effect of calcium additions on the oxidation behavior in magnesium alloys. *Scr. Mater.* **2000**, *42*, 1089–1094. [CrossRef]
22. Aydin, D.S.; Bayindir, Z.; Hoseini, M.; Pekguleryuz, M.O. The high temperature oxidation and ignition behavior of Mg–Nd alloys part I: The oxidation of dilute alloys. *J. Alloys Compd.* **2013**, *569*, 35–44. [CrossRef]
23. Kujur, M.S.; Mallick, A.; Manakari, V.; Parande, G.; Tun, K.S.; Gupta, M. metals Significantly Enhancing the Ignition/Compression/Damping Response of Monolithic Magnesium by Addition of Sm_2O_3 Nanoparticles. *Metals* **2017**, *7*, 357. [CrossRef]
24. Kujur, M.S.; Manakari, V.; Parande, G.; Tun, K.S.; Mallick, A.; Gupta, M. Enhancement of thermal, mechanical, ignition and damping response of magnesium using nano-ceria particles. *Ceram. Int.* **2018**, *44*, 15035–15043. [CrossRef]
25. Merson, D.; Vasiliev, E.; Markushev, M.; Vinogradov, A. On the corrosion of ZK60 magnesium alloy after severe plastic deformation. *Lett. Mater.* **2017**, *7*, 421–427. [CrossRef]
26. Tun, K.S.; Sripathy, A.P.; Tekumalla, S.; Gupta, M. materials Development of Novel Lightweight Metastable Metal-(Metal + Ceramic) Composites Using a New Powder Metallurgy Approach. *Materials* **2020**, *13*, 3283. [CrossRef] [PubMed]
27. Nguyen, Q.B.; Gupta, M. Enhancing compressive response of AZ31B magnesium alloy using alumina nanoparticulates. *Compos. Sci. Technol.* **2008**, *68*, 2185–2192. [CrossRef]